*J. Fluid Mech.* (1970), *vol.* 44, *part* 1, *pp.* 195–208
*Printed in Great Britain*



# The evolution of time-periodic long waves of finite amplitude

By O. S. MADSEN,† C. C. MEI

Department of Civil Engineering, Massachusetts Institute of Technology, Cambridge, Massachusetts

AND R. P. SAVAGE

Coastal Engineering Research Centre, U.S. Army Corps of Engineers, Washington, D.C.

(Received 24 February 1970)

The breakdown of shallow water waves into forms exhibiting several secondary crests is analyzed by numerical computations based on approximate equations accounting for the effects of non-linearity and dispersion. From detailed results of two cases it is shown that when long waves are such that the parameter $\sigma = \eta^* L^{*2}/h^{*3}$ is of moderate magnitude, either due to initially steep waves generated at a wave-maker or due to forced amplification by decreasing depth, waves periodic in time do not remain simply periodic in space. Numerical results are compared with experiments for waves propagating past a slope and onto a shelf.

## 1. Introduction

Recently, some experiments have been conducted at the Coastal Engineering Research Centre (C.E.R.C.) for time-periodic finite-amplitude long waves which do not break. In a horizontal channel, long waves generated at one end by a piston-type sinusoidal wave-maker are found to develop into forms that are not periodic in space (Galvin 1967, 1968). Beyond a certain distance from the wave-maker, secondary crests of decreasing amplitude and propagating at different speeds appear within a primary wavelength (as defined by linear theory). The phenomenon is observed within the range

$$0{\cdot}02 < \eta_0^*/h_0^* < 0{\cdot}2 \quad \text{and} \quad 0{\cdot}02 < h_0^*/L^* < 0{\cdot}09,$$

where $\eta_0^*$ (asterisks denoting a dimensional quantity) is half the wave height of the largest wave, $L^*$ is the wavelength according to linear theory and $h_0^*$ is the constant depth of water. In terms of the parameter, $\sigma_0 = \eta_0^* L^{*2}/h_0^{*3}$, characterizing the relative importance of amplitude and frequency dispersion, experiments were conducted within the range,

$$2{\cdot}5 < \sigma_0 < 500, \tag{1.1}$$

and generally speaking secondary crests appear sooner and in greater numbers for larger $\sigma_0$, with breaking occurring for the higher values ($\sigma_0 > \sim 100$).

† Present address: Coastal Engineering Research Centre, U.S. Army Corps of Engineers, Washington, D.C.

The observation by Savage (1967) that initially small sinusoidal waves broke down in a similar manner upon entering a shallow shelf suggested the disintegration to be inherent in the nature of long waves rather than being caused by some exterior mechanism such as, for example, higher harmonics in the motion of the wave-maker.

It should be noted that the secondary crests occur for waves so long that the side-band instability of Benjamin & Feir (1967) is ineffective (unstable if $h_0^*/L^* > 0{\cdot}216$ (Benjamin 1967)). In a classical paper, Korteweg & de Vries (1895) pointed out that long waves of finite amplitude with initially sinusoidal form will always become steeper at the front of the crest and flatter behind. While the front steepens, the effect of frequency dispersion (or vertical acceleration) becomes increasingly appreciable, which may lead to the development of undulations behind each crest. This mechanism has been clearly explained by Peregrine (1966) for the generation of undular bores, and is also responsible for the disintegration of a forward-leaning solitary crest (Madsen & Mei 1969, hereafter as I). Therefore it should be possible to predict quantitatively, from the same approximate equation used in (I), the features observed by Galvin and Savage. In fact, these equations ((2.4) and (2.5), I) derived under the assumption

$$\sigma = \eta^* L^{*2}/h^{*3} = O(1),$$

account for both non-linearity and dispersion and include as limiting cases the non-dispersive theory of Airy at one extreme, $\sigma \gg 1$, and the linearized shallow theory at the other, $\sigma \ll 1$. Hence they may be regarded as the most uniformly valid basis for shallow water waves so long as the wave slope remains small everywhere,

$$O(\eta^*/L^*), \quad O(h^*/L^*) < 1, \tag{1.2}$$

i.e. they are applicable to virtually all non-breaking or prebreaking waves. Airy's theory for long waves also bears the restriction (1.2), and hence its prediction of breaking merely suggests a possible tendency but does not correspond exactly to reality.

The purpose of this paper is to present detailed results calculated for two cases where secondary crests are a dominant feature: one for a horizontal bottom and one for a bottom sloping to a shallow shelf, and to compare calculated results for the second case with some records obtained from a large-scale experiment.

## 2. Governing equations and auxillary conditions

Reference is made to (I) for the basic form of the governing equations for the velocity variable, $u$, which is $1 + (h')^2$ times the horizontal velocity at the bottom $y = -h(x)$, and the free surface elevation $\eta$ [c.f. (2.4) and (2.5), I]. Recalling that they can be expressed in characteristic form along the double characteristic $dx/dt = 0$ as

$$d\eta/dt = v \quad \text{and} \quad dv/dt = a \tag{2.1}$$

and along the sloping characteristics

$$\frac{dx}{dt} = \pm C_0(x) = \pm \left[ \frac{3h}{\epsilon} \frac{1 - (h')^2 - hh''}{1 - \frac{1}{2}hh''} \right]^{\frac{1}{2}}, \quad \epsilon \equiv h_0^*/L^*, \tag{2.2}$$

as

$$(\tfrac{1}{6}Ch+\tfrac{1}{2}uh)\frac{d\eta}{d\beta}+\tfrac{5}{12}h^2h'\frac{dv}{d\beta}+(1-\tfrac{1}{2}hh'')\tfrac{1}{6}\epsilon hC^2\frac{du}{d\beta}+\tfrac{1}{12}\epsilon h^2C\frac{da}{d\beta}$$
$$=(\tfrac{1}{2}ChD+\tfrac{1}{6}\epsilon hCu)u+\tfrac{1}{6}hh'(\tfrac{5}{2}h-\epsilon C^2)a+[\tfrac{1}{2}\eta C-\tfrac{1}{3}hC+(\tfrac{1}{2}h+\tfrac{1}{6}\epsilon C^2)u]v, \quad (2.3)$$

where
$$D\equiv(h'/h)\eta-h'+(h')^3+\tfrac{1}{3}h^2h'''+2hh'h'' \quad (2.4)$$

and
$$C=\begin{bmatrix}+C_0(x)\\-C_0(x)\end{bmatrix} \quad \text{along} \quad \beta=\begin{bmatrix}\beta_1\\\beta_2\end{bmatrix}=\frac{1}{2}\left[t\mp\int\frac{dx}{C_0(x)}\right]=\text{const.} \quad (2.5)$$

All variables have been made dimensionless by the length scale $L^*$ and time scale $L^*/(gh_0^*)^{\frac{1}{2}}$. (Unless otherwise stated, variables used in this paper are dimensionless.)

Initially the water is assumed at rest, i.e.

$$\eta, v, a, u = 0 \quad t\leqslant 0, \quad x>0, \quad (2.6)$$

and waves are assumed to radiate from $x=0$ due to a disturbance at this point. Choosing this disturbance to be described as the boundary value of $\eta$ at $x=0$, i.e.

$$\eta(0,t)=f(t) \quad (t\geqslant 0), \quad (2.7)$$

we also have
$$v(0,t)=f'(t) \quad \text{and} \quad a(0,t)=f''(t), \quad (2.8)$$

since $x=0$ is a characteristic. These boundary conditions correspond to the surface variation as measured at a fixed point by a wave gauge, and the value of $u(0,t)$ is calculated from earlier time steps along the characteristic $\beta=\beta_2=$ constant. In this manner the initial boundary-value problem is consistently posed, and the numerical procedure is essentially the same as described in (I).

For our problem we choose

$$f(t)=\begin{cases}\eta_0[(6-2\pi^2)t^5+(4\pi^2-15)t^4+(10-2\pi^2)t^3] & (0\leqslant t\leqslant 1),\\ \eta_0\cos 2\pi t & (t\geqslant 1)\end{cases} \quad (2.9)$$

where the transition $(0\leqslant t\leqslant 1)$ is chosen to achieve smoothness at $t=0$ and 1. This boundary condition approximately describes the situation near a sinusoidal wave-maker, and as (2.9) implies, the time scale is the dimensional period $T^*$ of the 'wave-maker' and the length scale is the wavelength according to linearized long wave theory $L^*=T^*(gh_0^*)^{\frac{1}{2}}$.

## 3. Horizontal bottom

Calculations show that for $\sigma_0<5$ the waves remain nearly sinusoidal in space for a long distance from $x=0$, in qualitative agreement with the observations of Galvin. The comparison made in this section with Galvin's experiments is limited to gross features, partly because viscosity seems to be important in his experiments (typical depth was 0·5 ft) and partly because the assumed boundary condition only approximates that corresponding to a sinusoidal wave-maker. In order to accentuate the development of irregularity we selected the case where $\eta_0=\frac{1}{4}h_0$, $\epsilon=h_0=\frac{1}{16}$ so that $\sigma_0=\eta_0/h_0^3=64$. Figure 1 depicts the instantaneous surface profile approximately eight periods after the initiation of motion, i.e.

$t > 8$. Secondary crests appear immediately downstream of $x = 0$. As many as three crests of different heights can be identified within a primary wavelength ($16h_0$), in agreement with Galvin's (1967) experimental results. The leading disturbance appears to be separated from the rest as a solitary wave of amplitude $= 0{\cdot}35h_0$ and moving with the corresponding speed. Numerical accuracy is checked for mass balance excluding the leading waves. Near the wave-maker the evolution clearly resembles the disintegration of a solitary wave entering a shelf as reported in (I).

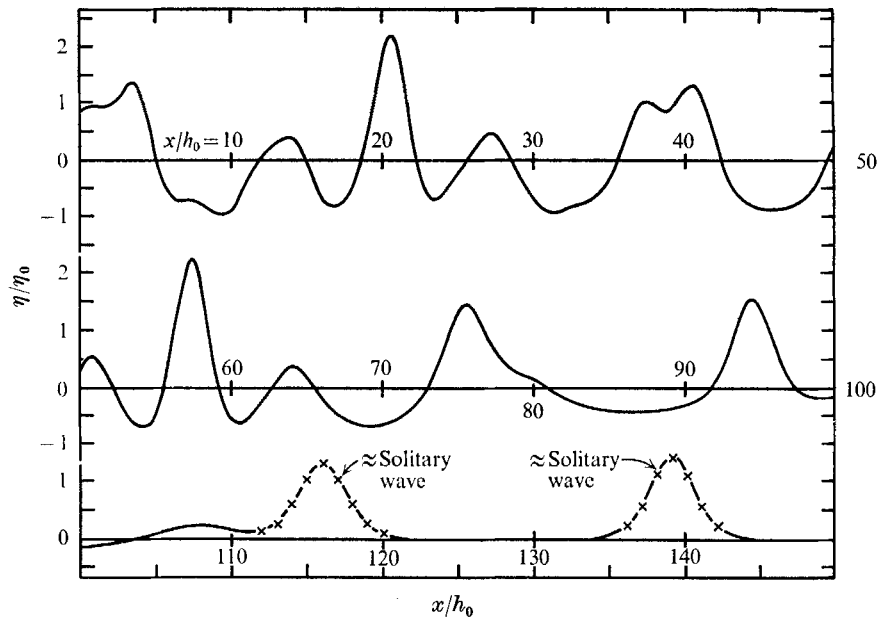


FIGURE 1. Surface profile shortly after the eighth period since the initiation of motion. Theoretical solitary wave profile for the same crest height ( × ).

The trajectories of the largest two crests within each primary wavelength are shown in the $x,t$ diagram in figure 2. From approximately $t > 4$ onward a quasi-steady, time-periodic state is established for all $x/h_0 < 50$; the time interval between the arrival of successive peaks of the same family is precisely one. Except when the two crests are close their traces are straight and of constant slope. The wave speeds, as calculated from the slopes of the traces, are 1·08 and 0·86 for the largest (primary) and the second largest peaks respectively. The fact that the wave speed of the secondary crest is less than unity suggests that it is not a solitary wave, which would move faster than unity on the present scale. As the spatial separation between two successive peaks of the same family is also constant, it is at least convenient to consider these crests as belonging to separate wave trains with definite speeds and lengths.

It is interesting to note the events when a primary crest closes in on the preceding secondary crest from behind. During the approach, the larger crest decreases in height while the smaller one increases. The two, however, do not actually pass through each other; instead they attain equal height when they

are still at a finite distance apart. Then they exchange roles in both amplitude and speed and begin to separate from each other (figure 3). Similar results have been discovered by Zabusky (1967) for two solitary waves of quite different heights (height ratio = 2·25).

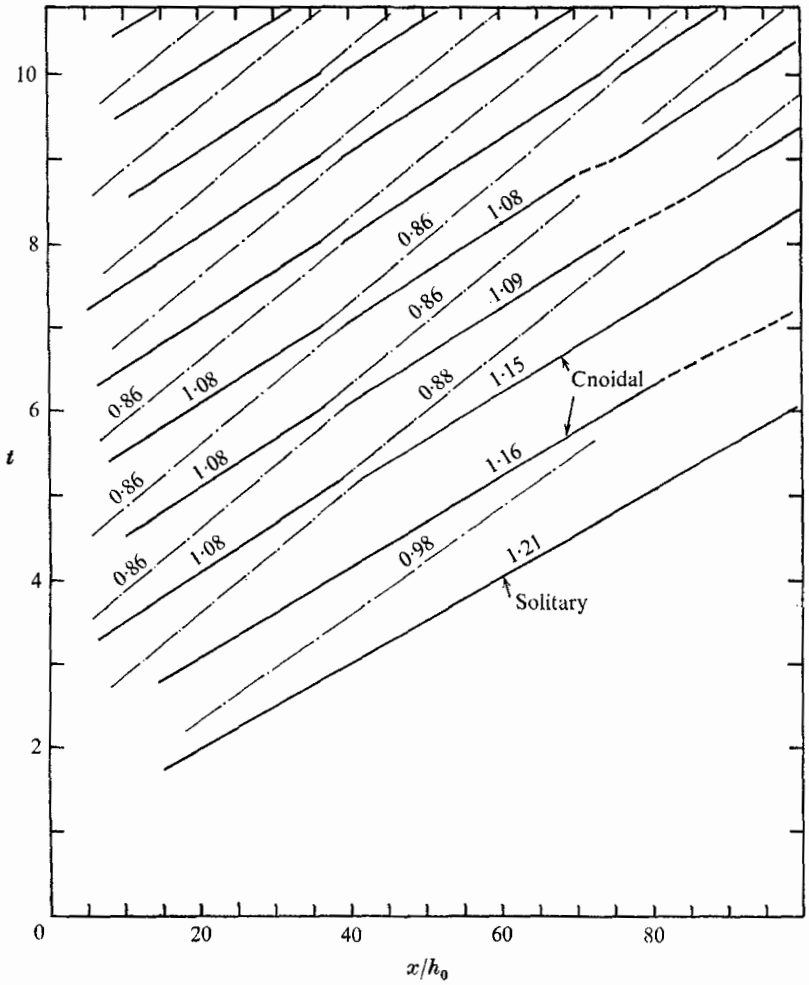


FIGURE 2. Trajectories of the largest two peaks (primary and the largest secondary) into which each generated wave disintegrates. ——, primary; —·—·, largest secondary; – – – –, only one peak identifiable. Numbers indicating $dx/dt$.

To follow the variation of amplitude, the envelope of the primary crest can be traced. It is found that the envelope is itself periodic in time and space with the wavelength = $38h_0$, i.e. roughly twice the linear wavelength (figures 4 and 5). The waviness in the envelope is most likely due to the third or even smaller crests. This 'beat' phenomenon, also observed by Galvin (1967), is not surprising given the existence of wave trains with different wavelengths and speeds.

Near the leading disturbance behind the transients, the primary crests shed off the smaller ones and eventually emerge as a wave train periodic in both space

and time. Upon comparison with the classical theory this purely periodic state is seen to be essentially the cnoidal wave (see the comparison in figure 6 where the result for a different case is also given). We shall give some evidence suggesting

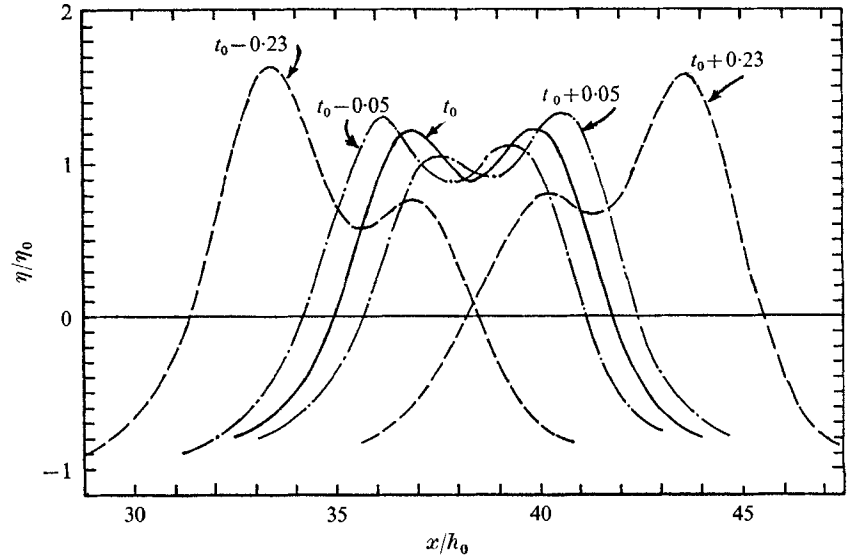


FIGURE 3. Exchange of roles between the largest two peaks.

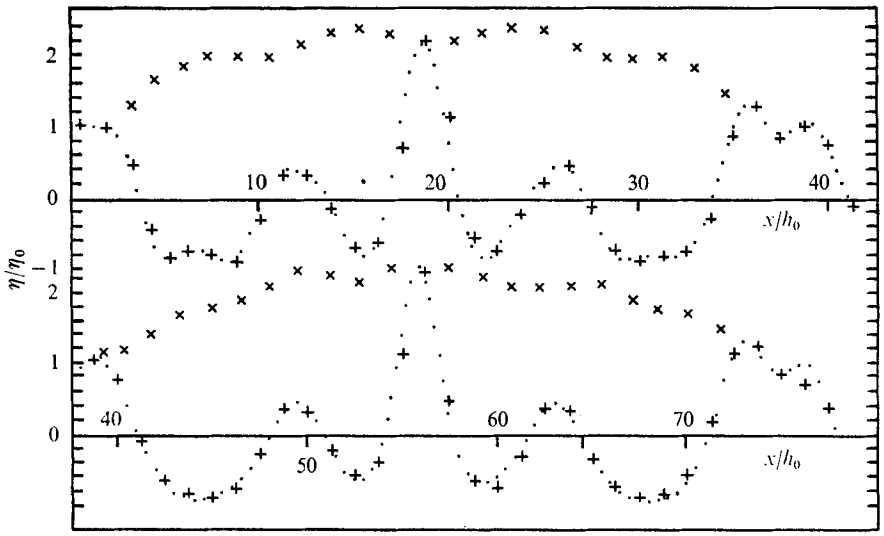


FIGURE 4. The temporal periodicity and the 'beat' phenomenon; + +, $t = 9{\cdot}02$; ····, $= 10$; × ×, envelope of the highest crest.

that the complex motion between the cnoidal waves near the front and the wave-maker may be considered as weakly interacting cnoidal wave trains. Consider again only the wave trains associated with the two largest crests (primary and the largest secondary). When a primary peak is midway between two secondary

peaks it is superimposed on the negative velocity field associated with the trough of the secondary waves. Hence, a reduction in speed and an increase in amplitude must take place. Similarly, when a secondary peak is midway between two

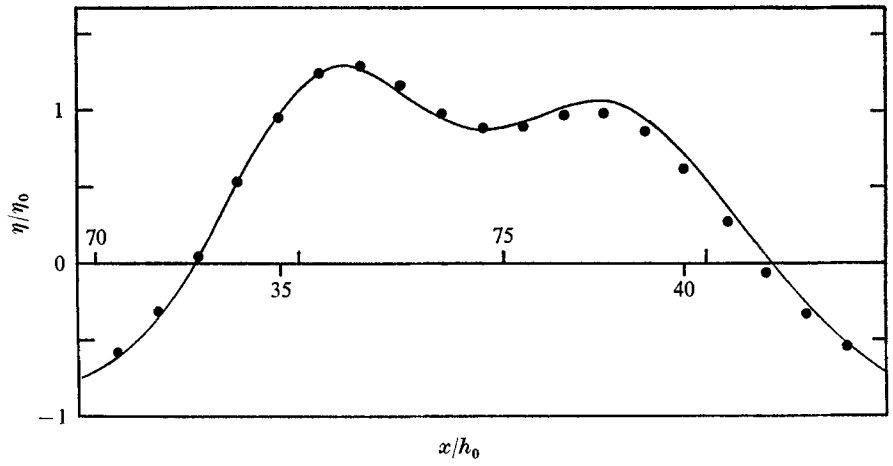


FIGURE 5. The spatial periodicity of beats at $t = 10$: ——, profile near $x/h_0 = 38$; · · · ·, near $x/h_0 = 75$.

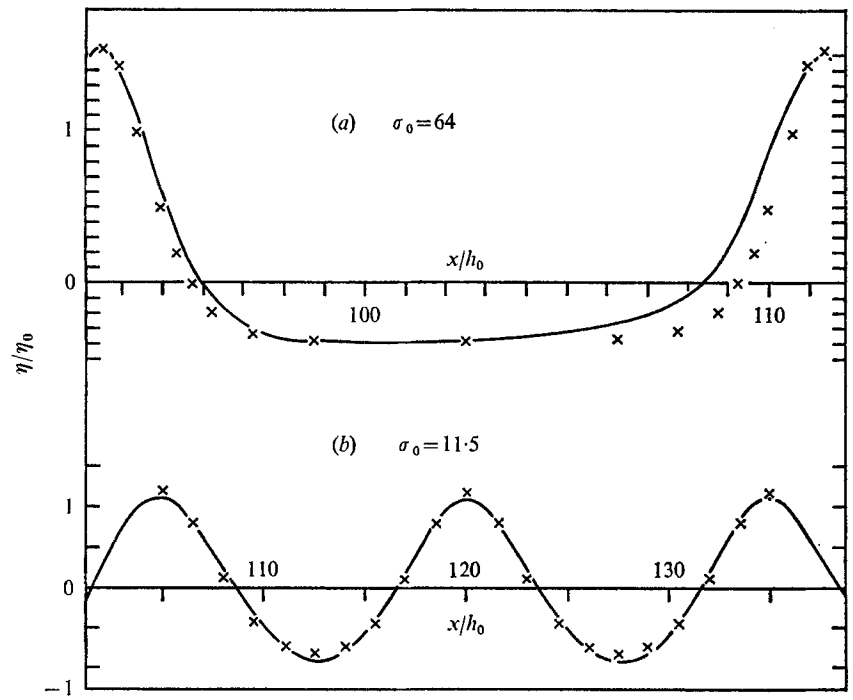


FIGURE 6. Comparison between profiles of cnoidal waves ( × ) and computed waves when primary peaks have outrun the secondaries (——). Corresponding comparison of wave speeds between cnoidal theory ($C_{\text{th}}$) and computation ($C_{\text{co}}$). Case (*a*) $C_{\text{th}} = 1{\cdot}16$, $C_{\text{co}} = 1{\cdot}15 \sim 1{\cdot}16$; case (*b*) $C_{\text{th}} = 0{\cdot}99$, $C_{\text{co}} = 0{\cdot}98$.

primaries, its speed is reduced and its amplitude increased. Based on this idea, a crude first-order estimation of the wave speeds for each train, assumed individually cnoidal, can be made. This is done in table 1. Since the estimated wave speeds are reasonably close to the computed ones, it appears that the assumption of the complex motion being that of two cnoidal wave trains interacting nearly linearly with each other is reasonably supported.

| | Primary wave | Largest secondary wave |
|---|---|---|
| Estimated total height when isolated: $\eta_{cr} - \eta_{tr}$ | $0{\cdot}47h_0$ | $0{\cdot}15h_0$ |
| Trough amplitude according to cnoidal wave theory: $\eta_{tr}/h_0$ ($\approx$ mean fluid velocity under trough by linearized theory $\bar{u}$) | 0·09 | 0·06 |
| Estimated speed of propagation = cnoidal wave speed − mean fluid velocity at trough of the other wave | 1·10 | 0·93 |
| Propagation speed by computation | 1·08 | 0·86 |

TABLE 1

## 4. Periodic waves on a shelf

In 1967 an experiment was made at the Coastal Engineering Research Centre in which waves were generated in the deep region of a tank, travelled over a sloping bottom and advanced into shallower water of a shelf. The periodic wave in deeper water was essentially sinusoidal, but the parameter, $\sigma$, was amplified by the reduction in depth, such that on the shelf this was no longer small, and secondary crests developed as the wave travelled down the shelf. Since the experiments were conducted on a sufficiently large scale to reduce the effect of damping substantially, the results afford a direct check of the frictionless theory. Therefore, calculations were made corresponding exactly to the experiments, except that the shelf was assumed to be infinitely long.

### (*a*) *Experimental procedure*

The experiments were performed in the large outdoor tank at C.E.R.C. (see figure 7). The tank is 635 ft. long, 20 ft. deep and 15 ft. wide. A concrete slope (1:15) was constructed to provide a transition between two horizontal bottoms. The water depth was maintained at 8 ft. in the deeper section ($h_0^*$) and 2 ft. on the shelf ($h_1^*$). At the end of the deep section ($x = 0$), waves of 4 sec period were generated by a flap-type generator hinged at the bottom; the corresponding characteristic length is $L^* = T^*(gh_0^*)^{\frac{1}{2}} = 64$ ft. $= 8h_0^*$. For a stroke amplitude of 2 ft. measured at 20 ft. above the bottom, the wave amplitude near the flap was $\eta_0^* = 0{\cdot}32$ ft. The shelf ended in a very efficient crushed-stone absorber.

Measurement of the wave profile was made at a number of stations along the tank, the general procedure at every station was to calibrate a parallel-wire resistance wave gauge, then to start the wave generator and to record the passage

of the first 20 or 30 waves. The same gauge was then moved to the next station and the whole procedure repeated. The profile was recorded at 50 ft. intervals in the deep portion and at 1 ft. intervals over the slope and the shelf. Wave speeds were not measured.

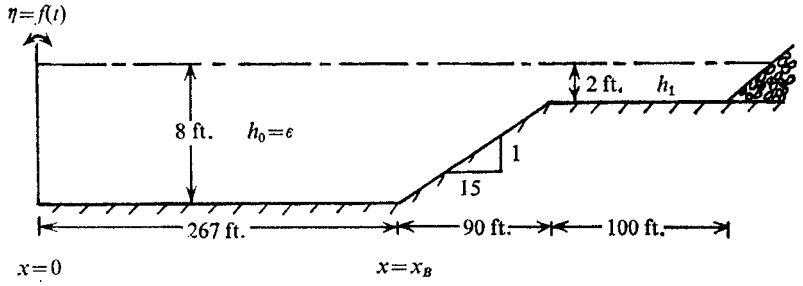


FIGURE 7. Experimental configuration for C.E.R.C. outdoor wave tank tests.

### (*b*) *Comparison of computed and measured results*

The waves generated in the deep region correspond to $\sigma_0 = 2{\cdot}5$ and should remain sinusoidal over the distance under consideration. In principle, some reflexion must be caused by the beach, which will eventually affect the boundary condition at $x = 0$. Theoretical estimation according to linearized long wave theory (see, for example, Kajiura 1961 or Madsen 1969) shows that the reflexion coefficient for the present parameters is less than two percent; this is also supported by experimental records. Thus $x_B$ was chosen as $12{\cdot}5h_0$ to save computation time.

The transformation on the beach is examined for crest and trough amplitudes (figure 8). The agreement between experiments and the calculations is good. Also, figure 8 shows that the trough height changes little along the slope and that, as the depth decreases, the crest to trough amplitude (wave height) is underestimated by the linear wave theory.

On the shelf the main crest amplitude is nearly doubled, and the parameter $\sigma_1$ rises to about 41. Thus, the secondary crests are generated at once. Figure 9 shows the surface profile as the ninth wave crest enters the shelf. It can be seen that at the front (in an imaginary extension of the actual tank) a zone of cnoidal waves of amplitude $0{\cdot}36h_1$ has already appeared ahead of the zone of multiple crests. Upon checking the mass conservation, it is found that the mean water level over the shelf has dropped by about $\Delta h/\eta_0 = 0{\cdot}039$. This feature is also present when a Stokes wave is incident upon a slowly varying bottom; it is the result of a steady momentum flux in waves which must be balanced by an adjustment in hydrostatic pressure. According to a formula by Longuet-Higgins & Stewart (1962) (see Phillips 1966, p. 55), the corresponding drop for the Stokes waves would be 0·066. A different calculation for long waves with reduced amplitude such that $\eta_0/h_0 = 0{\cdot}025$ gives $\Delta h/\eta_0 = 0{\cdot}0375$ in comparison with 0·041 for the Stokes waves.

Detailed comparisons of wave profiles from experiments and calculations are shown in figure 10 for the four stations indicated in figure 9. In these figures the time axis does not represent the absolute time from the start of the wave-maker.

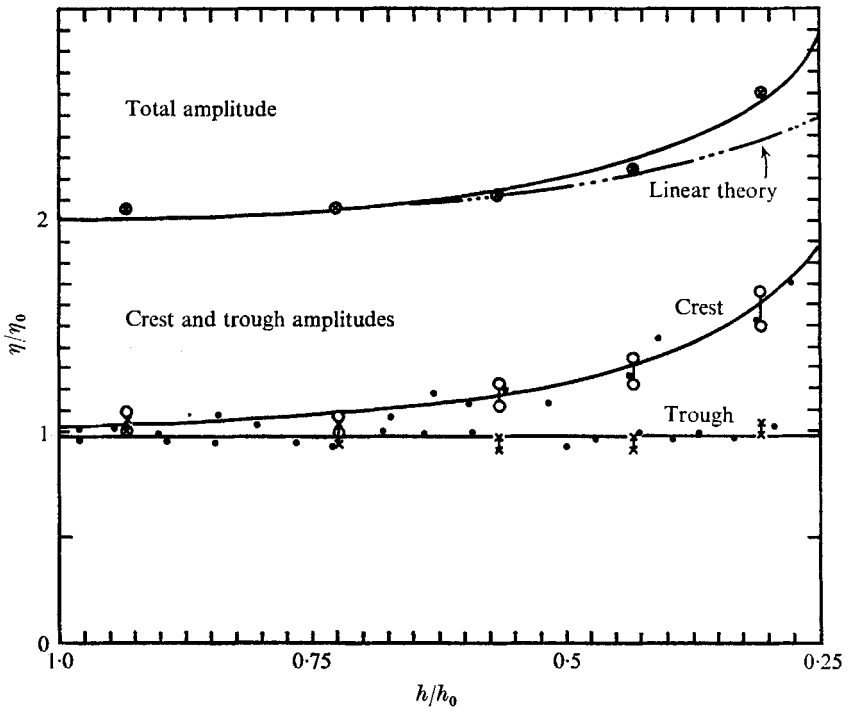


FIGURE 8. Amplitude variation of a periodic wave during shoaling. Experiments: O—O, crest; × — ×, trough; ⊗, averaged total amplitude from crest to trough. ——, present theory.

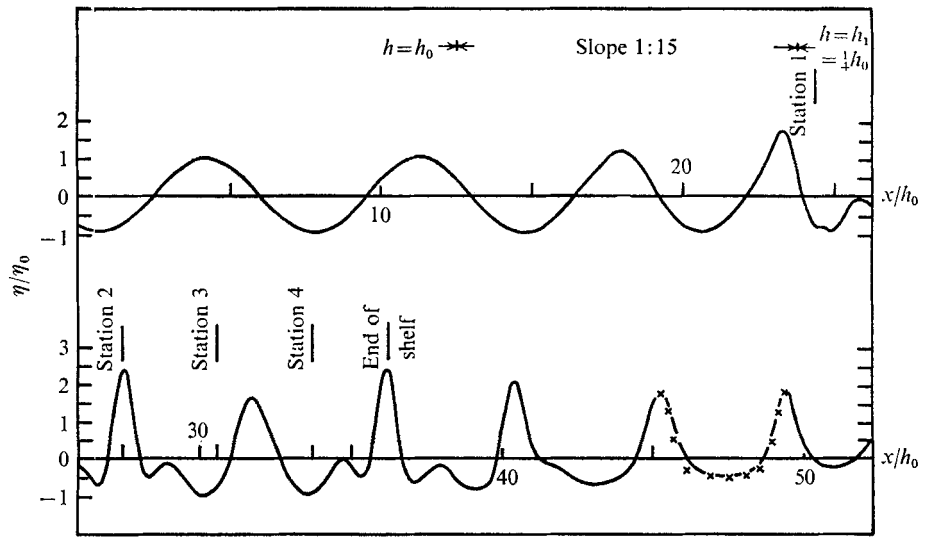


FIGURE 9. Surface profile after twelfth period of wave-maker. ×, profile of cnoidal wave of equal height.

Rather, for each station $n$, $n = 1, 2, 3, 4$, we examine the time range where steady state is already reached in both theory and experiment, and compare the profiles for a typical period by fitting the time instant $t_n$ corresponding to the first passage of a crest. The general agreement at the first two stations seems unmistakable;

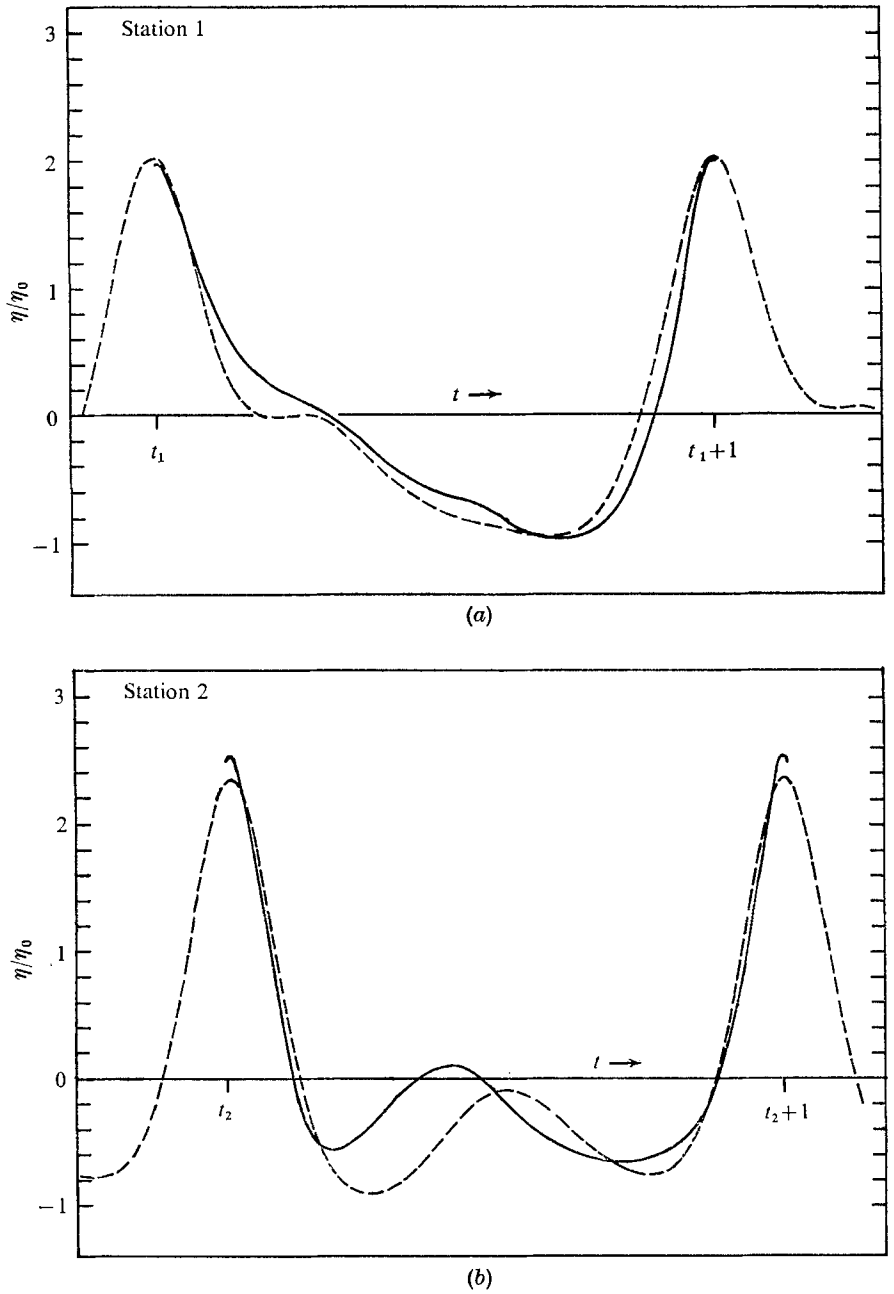


FIGURE 10. Comparison for a typical period between computed (– – –) and experimental (——) profiles at various stations on the shelf. Location of stations is indicated in figure 9.

however, the development of the secondary crest is somewhat prematurely predicted by the computed profiles. Thus at stations 3 and 4 the theoretical interaction between the smaller and larger crests is more advanced than that shown by the experiments. This explains the discrepancy in amplitude of the larger

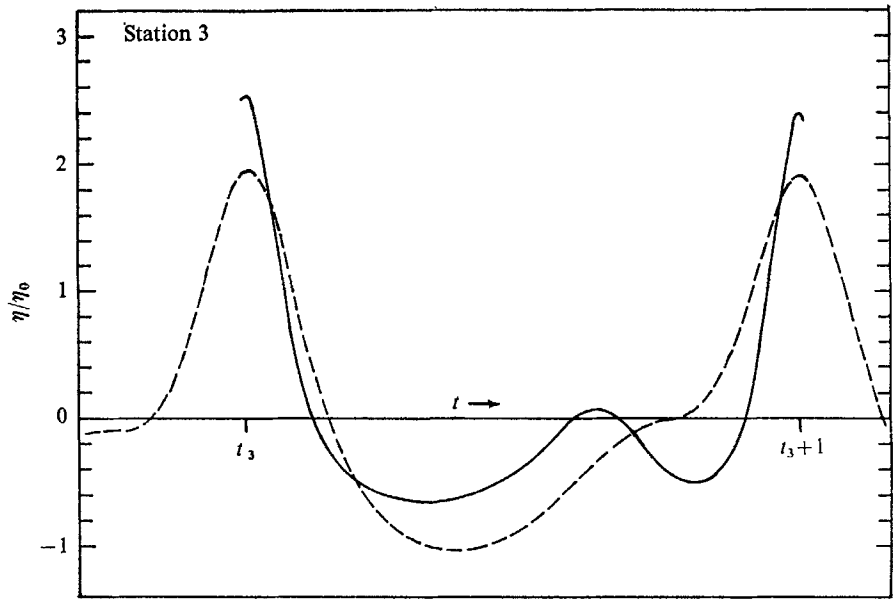


(*c*)

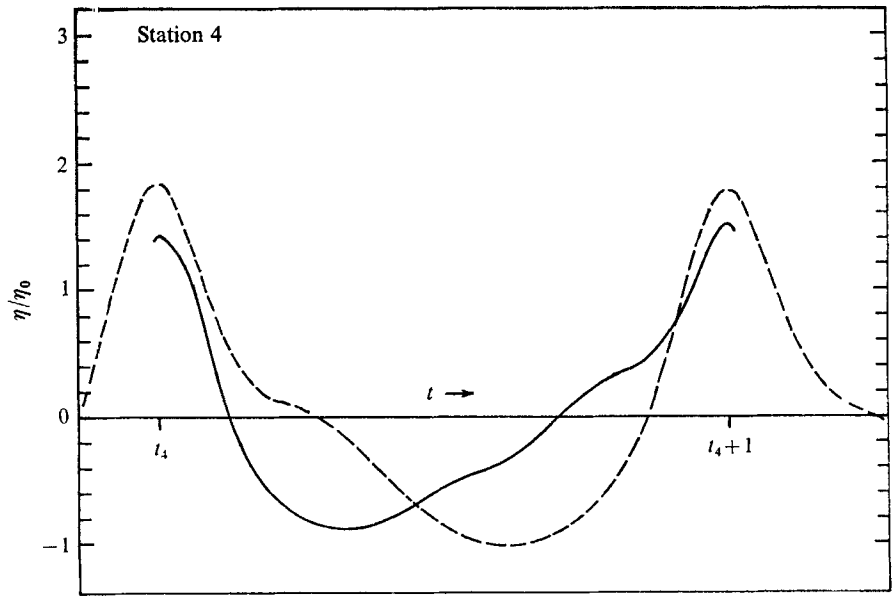


(*d*)

FIGURE 10(*c*), (*d*). For legend see p. 205.

crests. We attribute this gradual deviation to frictional retardation. In partial support of this explanation, figure 11 shows that the experimental record taken at station 4 compares fairly well with the calculated results for a station midway between stations 3 and 4.

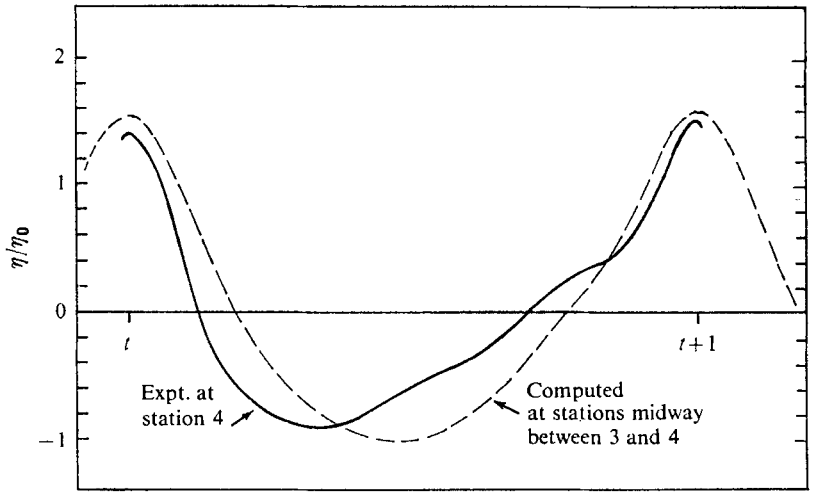


FIGURE 11. Illustration of the slower development in experiment.

## 5. Concluding remarks

The results presented in the previous sections exhibit the occurrence of the secondary crests as a dominant feature. In the constant-depth case the resulting profiles indicated that when waves are generated and travel under the conditions assumed, the total wave train transforms into three regions. The leading region will be a train of essentially solitary waves followed by a region of cnoidal waves. The third region, that nearest the generator, appears to be a region of weakly interacting cnoidal wave trains.

The computed profiles of waves travelling over a slope and onto a shelf compare well with available experimental data, but appear to predict an earlier development of secondary crests than shown by experiments. It is believed that the difference can be explained by frictional effects in the experiments, but so far no conclusive proof of this is available.

The numerical work was supported by the Office of Naval Research, U.S. Navy through Contract NONR 1841(59) with the Hydrodynamics Laboratory, Massachusetts Institute of Technology. The experimental data were collected as part of the research programme of the U.S. Army Corps of Engineers, Coastal Engineering Research Centre.

## REFERENCES

BENJAMIN, T. B. 1967 *Proc. Roy. Soc.* A **299**, 59.

BENJAMIN, T. B. & FEIR, J. E. 1967 *J. Fluid Mech.* **27**, 417.

GALVIN, C. J. 1967 *Internal report, Coastal Engineering Research Center.*

GALVIN, C. J. 1968 Abstract in *Trans. Am. Geoph. Union*, **49**, 206.

KAJIURA, K. 1961 *Tsunami Committee, Int. Union Geology and Geophysics Monograph*, no. 24.

KORTEWEG, D. J. & DE VRIES, G. 1895 *Phil. Mag.* (5), **39**, 422.

LONGUET-HIGGINS, M. S. & STEWART, R. H. 1962 *J. Fluid Mech.* **13**, 481.

MADSEN, O. S. 1969 Sc.D. Thesis, Massachusetts Institute of Technology.

MADSEN, O. S. & MEI, C. C. 1969 *J. Fluid Mech.* **39**, 781.

PEREGRINE, D. H. 1966 *J. Fluid Mech.* **25**, 321.

PHILLIPS, O. M. 1966 *The Dynamics of the Upper Ocean.* Cambridge University Press.

SAVAGE, R. P. 1967 Unpublished report of U.S. Army Corps of Engineers, Coastal Engineering Research Centre.

ZABUSKY, N. J. 1967 In *Nonlinear Partial Differential Equations* (ed. W. F. Ames). New York: Academic.